

Flipping interferometry and its application for quantitative phase microscopy in a micro-channel

DARINA ROITSHTAIN,¹ NIR A. TURKO,¹ BAHRAM JAVIDI,² AND NATAN T. SHAKED^{1,*}

¹Department of Biomedical Engineering, Faculty of Engineering, Tel Aviv University, Tel Aviv 69978, Israel

²Department of Electrical and Computer Engineering, University of Connecticut, Storrs, Connecticut 06269-4157, USA

*Corresponding author: nshaked@tau.ac.il

Received 2 February 2016; revised 15 April 2016; accepted 15 April 2016; posted 19 April 2016 (Doc. ID 258702); published 12 May 2016

We present a portable, off-axis interferometric module for quantitative phase microscopy of live cells, positioned at the exit port of a coherently illuminated inverted microscope. The module creates on the digital camera an interference pattern between the image of the sample and its flipped version. The proposed simplified module is based on a retro-reflector modification in an external Michelson interferometer. The module does not contain any lenses, pinholes, or gratings and its alignment is straightforward. Still, it allows full control of the off-axis angle and does not suffer from ghost images. As experimentally demonstrated, the module is useful for quantitative phase microscopy of live cells rapidly flowing in a micro-channel. © 2016 Optical Society of America

OCIS codes: (090.1995) Digital holography; (180.3170) Interference microscopy; (100.3175) Interferometric imaging; (170.3880) Medical and biological imaging.

<http://dx.doi.org/10.1364/OL.41.002354>

Quantitative imaging of biological cells during flow is useful for medical diagnosis based on cell sorting and other biological assays [1,2]. This task, however, typically requires very rapid image acquisition capabilities to allow fast cell flow for analyzing a sufficient number of cells. In this scenario, no scanning or multiple camera exposures per sample instance is allowed. Wide-field interferometric phase microscopy (IPM) in off-axis geometry is useful for quantitatively imaging rapidly moving transparent samples, such as biological cells during flow, without the need for labeling. This is done by capturing the two-dimensional (2D) optical path delay (OPD) map of the sample, taking into consideration both the cell thickness and its refractive index content [3]. To obtain the OPD map, IPM creates on the camera interference between the light passing through the sample and a reference beam that does not contain spatial sample information. A small off-axis angle is induced between the beams to allow the OPD map reconstruction from a single camera exposure.

Historically, IPM was based on interferometers built around the sample, where splitting to sample and reference beams was carried out before interacting with the sample. This technique, however, is subject to noise because of differential environmental effects between the beams. In common-path interferometers

the interfering beams share a large part of the optical path, so that time-dependent differential noise is minimized. Part of these interferometers, however, require specialized optical elements, such as diffraction gratings [3–5], polarization control [6,7], or an additional microscope objective in the beam path [8], which may make the system more bulky, harder to align, or limit it to image non-birefringent samples.

Shearing interferometers are close-to-common-path interferometers that create two laterally sheared sample beams, superimposed at the camera plane. Depending on the amount of shearing and the density of the sample, quantitative phase microscopy is possible by shearing interferometry. Most shearing interferometers, however, cannot image dense samples. This occurs due to the creation of ghost images, which originate from different imaging information that exist at the same spatial locations in the two sheared beams [6,9–12]. In addition, simplified and highly compact shearing interferometers cannot control the off-axis angle between the sample and reference beams, because the lateral shearing distance and the off-axis angle are coupled. Removing the sample information from one of the beams [3,4,13,14] allows imaging dense samples, at the cost of using spatial filtering in the interferometric module, typically requiring a difficult pinhole alignment.

In this Letter, we propose the flipping interferometry (FI) module for off-axis close-to-common-path IPM. This module is highly compact, cost effective, and easy-to-implement and to align. When using this module, the underlying assumption is that the optical field of view (FOV), meaning the beam spot size in the camera plane, is at least twice as wide as the digital FOV, meaning the size of the camera sensor. This condition is valid in most microscopy setups. Figure 1(a) presents a scheme of an inverted microscope, illuminated by a coherent laser (Helium–Neon, 632.8 nm). The beam passes through the sample, is magnified by a microscope objective (Newport, 60 \times , 0.85 NA), and projected through a tube lens ($f = 150$ mm) onto the digital camera (Thorlabs, DCC1545M). The proposed FI module is positioned between the tube lens and the camera, such that the camera is positioned in the image plane of the sample. In this module, the magnified sample beam is split by the beam splitter (BS) into two beams. One beam propagates toward a slightly tilted mirror (M_1), and is reflected back to the camera in an off-axis angle. The other beam from the BS

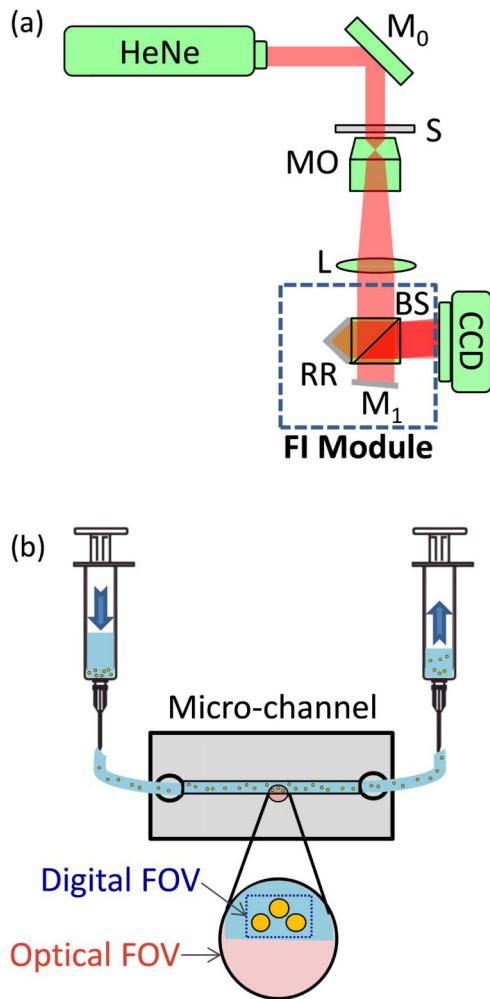


Fig. 1. (a) An inverted microscope illuminated by a Helium–Neon (HeNe) laser, where the FI module is positioned between tube lens L and the CCD camera. M_0 , M_1 , mirrors; S, sample; MO, microscope objective; BS, beam splitter; RR, retro-reflector. (b) A micro-channel, positioned in the sample plane for interferometrically imaging cells during flow. For FI, the optical FOV is chosen at the side of the channel, so that one half of the optical FOV is empty.

propagates toward a retro-reflector (RR), which is built using a pair of mirrors, attached to each other in a 90 deg angle. Alternatively, the mirror RR can be integrated with the BS faces to avoid redundant free-space propagation.

If we position a screen at the camera plane, and it is larger than the beam spot, we obtain two off-axis interferograms, each of which is on one half of the optical FOV. If one half of the original optical FOV is not occupied, it can be considered as the reference beam for the other half of the optical FOV. This scenario is easily met in imaging samples containing micro-fluidic channels for flowing biological cells, as shown in Fig. 1(b). In optical microscopy, the digital camera sensor size, defining the digital FOV, is typically much smaller than the optical FOV. Therefore, provided that the camera sensor is positioned on one of the sides of the optical FOV, an off-axis interferogram of the sample is created on the digital camera.

We first used a 1951 US Air Force (USAF) resolution target to demonstrate experimentally the principle of operation of the

proposed FI module. As shown by the red circle in Fig. 2(a), we chose an area on the test target that did not contain details to its right, which resulted in half of optical FOV without spatial sample information, as shown in Fig. 2(b). Figure 2(c) demonstrates the beam tracing and the creation of the image inside the FI module. As shown in this image, half of the optical FOV becomes the reference of the other half of the optical FOV. Therefore, on a screen positioned in the output plane, we experimentally obtained the flipped intensity image shown in Fig. 2(d) as a result of the reflection from the RR only, that is, by blocking the path to mirror M_1 in the FI module. Similarly, the non-flipped intensity image shown in Fig. 2(e) is a result of the reflection from mirror M_1 only, that is, by blocking the path to RR in the FI module. By letting both interferometric arms be active, we obtain the superimposed image shown in Fig. 2(f), and the red rectangle indicates the digital FOV, where the camera sensor is positioned. The

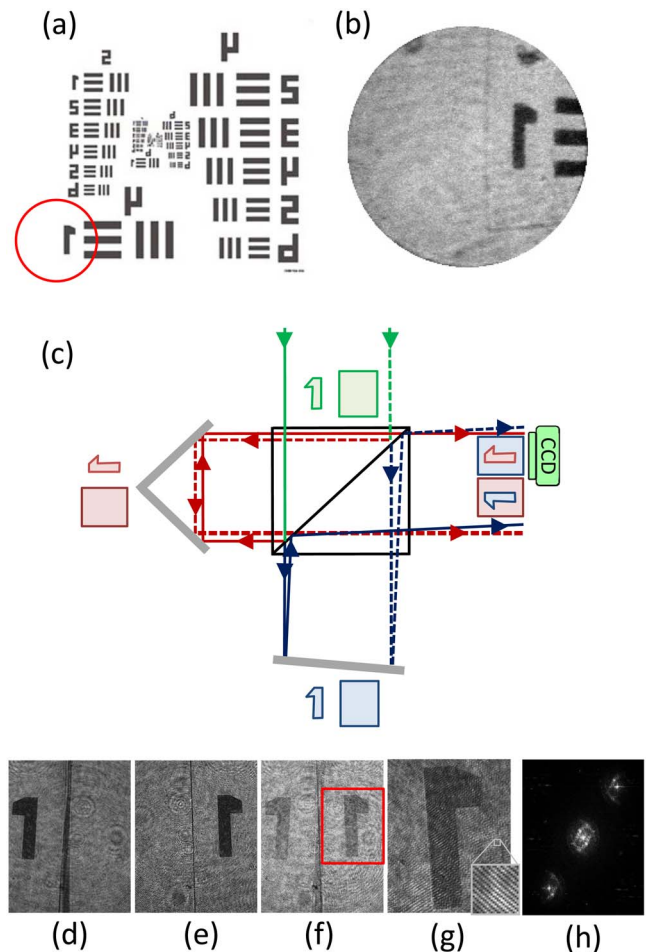


Fig. 2. Experimental demonstration of the principle of operation of the proposed FI method. (a) A 1951 USAF resolution target used as the sample, where the red circle indicates the optical FOV. (b) The full optical FOV on the digital camera plane. (c) Beam tracing and the creation of the overlapping images inside the FI module. (d) The optical FOV reflected back from the RR (mirror arm is blocked). (e) The optical FOV reflected back from the mirror (RR arm is blocked). (f) The optical FOV when no arm is blocked. The red rectangle indicates the digital FOV, where the camera sensor is positioned. (g) The off-axis interference pattern obtained on the digital camera. (h) The power spectrum of the off-axis interference pattern.

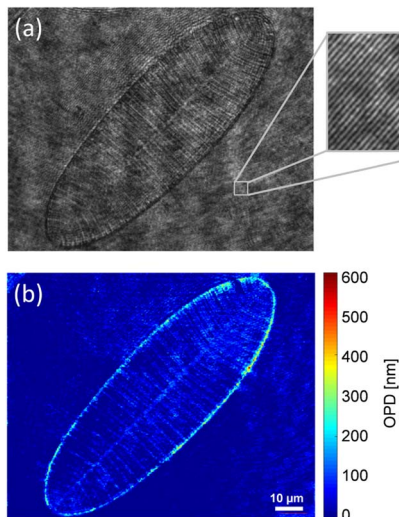


Fig. 3. Quantitative phase microscopy of unlabeled diatom shells using the FI module. (a) Off-axis interferogram. (b) Reconstructed OPD map.

camera finally records the off-axis image interferogram shown in Fig. 2(g), containing high-frequency spatial fringes with the spatial frequency controlled by the tilt of mirror M_1 in relation to the RR. The power spectrum of the off-axis interferogram, obtained by digital Fourier transform, is shown in Fig. 2(h).

As mentioned before, the proposed off-axis, close-to-common-path FI module has the advantages of compactness, ease of alignment, low degree of temporal noise, and low cost. It

can be made as small as the size of the BS, less than 3.5 cm. Specifically, in contrast to the interferometric module proposed in Ref. [8], our module does not contain an additional microscope objective that would make the system more bulky, expensive, and harder to align. In contrast to the simplified interferometric module proposed in Ref. [9], in the proposed FI module, the off-axis angle between the sample and the reference beams is not directly related to the beam shearing distance, and thus, provided that one half of the optical FOV is not occupied, our module does not suffer from ghost images with negative phase in the imaged FOV, which may prohibit imaging non-sparse samples (for example, highly confluent monolayer of cells). In addition, our module allows full control of the off-axis angle, to optimally fit the fringe spatial frequency to the camera pixel size.

To extract the quantitative phase maps from the off-axis interferograms, we used the off-axis Fourier-based algorithm [15], which includes a 2D Fourier transform, filtering one of the cross-correlation terms, and an inverse 2D Fourier transform, where the argument of the resulting matrix is the wrapped phase. To compensate for stationary aberrations and field curvatures, we subtracted from the wrapped phase the wrapped phase extracted from an interferogram acquired with no sample. We then applied the unweighted least squares phase unwrapping algorithm to resolve 2π phase ambiguities [16]. The resulting unwrapped phase map is multiplied by the wavelength and divided by 2π to obtain the quantitative OPD map of the sample.

We first acquired off-axis interferograms and measured the OPD stability of the highly coherent system, with resulting

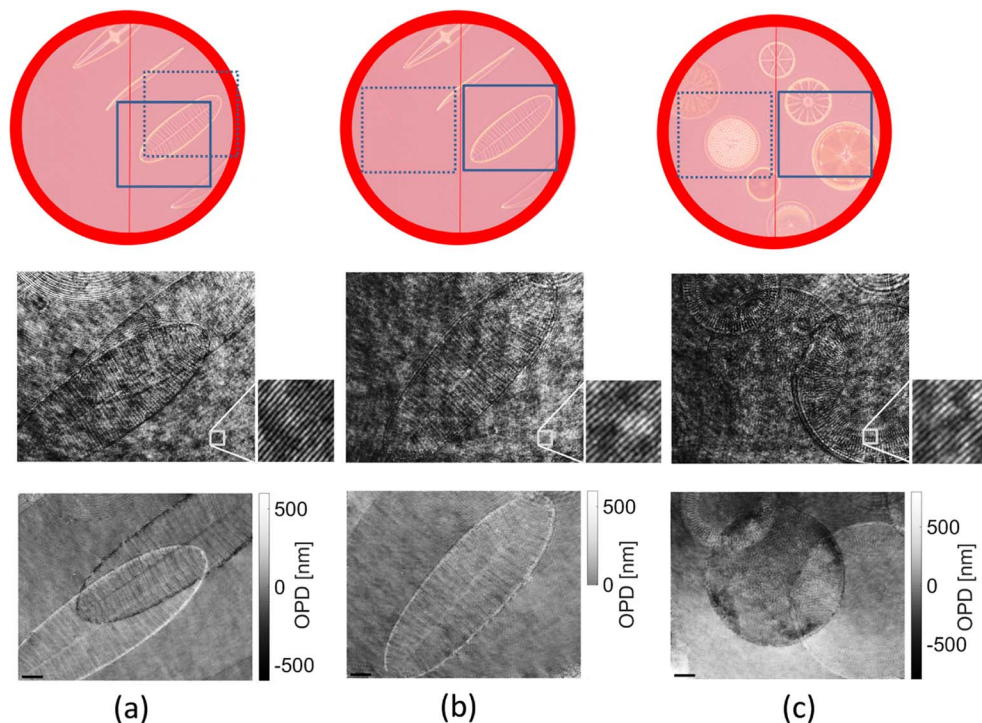


Fig. 4. (a), (b) Comparison between Kemper's method [9] in (a) and our FI method in (b), where half of the optical FOV is empty. (c) Our method, where the entire optical FOV is occupied. The first row of images shows bright-field images of the full optical FOV. The solid-line rectangle indicates the sample digital FOV, where the camera is located, and the broken-line rectangle indicates the reference FOV. The second row of images shows the off-axis interferograms acquired in these cases. The third row of images shows the reconstructed OPD maps in these cases. Scale bars on the bottom left side of the images represent 10 μm .

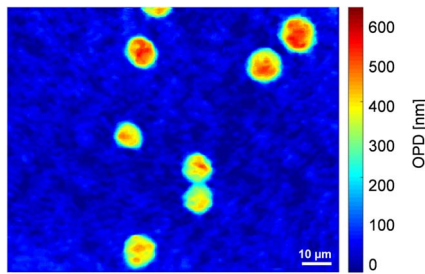


Fig. 5. Quantitative phase microscopy of live unlabeled cancer cells, rapidly flowing in a micro-channel as acquired by the FI module with the optical FOV located at the side of the channel. The coinciding video is shown in [Visualization 1](#).

temporal OPD stability of 0.85 nm. Next, we demonstrate using the FI module for quantitative phase microscopy of microscopic diatom shells, which are located on a slide so that the entire digital FOV is occupied, but still half of the optical FOV is not occupied and can be used as the reference beam to the other half of the optical FOV. The resulting off-axis interferogram is shown in Fig. 3(a). Figure 3(b) shows the final OPD map of the diatom shell obtained by processing the off-axis interferogram shown in Fig. 3(a).

For comparison, we experimentally implemented Kemper's shearing interferometric module [9]. Figures 4(a) and 4(b) present the results obtained for quantitative phase microscopy of microscopic diatom shells using this shearing interferometer and using our FI method. The spatial interference fringe frequency and the other experimental conditions were kept the same in both cases. As shown in Fig. 4(a), due to the decoupling between the off-axis angle and the overlapping FOVs, conventional shearing interferometry might induce overlapping positive and negative (ghost) phase images originated from the same sample features. Therefore, this method is less adequate for samples that are not sparse enough and occupy most of the digital FOV. On the other hand, as presented in Fig. 4(b), the FI module can cope with non-sparse or large samples that occupy most of the digital FOV, provided that the other half of the optical FOV is empty. As shown in Fig. 4(c), even the FI module will induce positive and negative overlapping phase images if the optical FOV is completely occupied.

As demonstrated in Fig. 1(b), the condition of using one half of the optical FOV as a reference beam is easily met when imaging micro-fluidic channels by controlling the lateral position of the sample in relation to the microscope objective and ensuring half empty optical FOV at the side of the channel. To demonstrate this experimentally, we quantitatively imaged MDA-MB-468 breast cancer cells during rapid flow in a micro-channel. Cells were grown in Roswell Park Memorial Institute (RPMI) medium until 80% confluence was achieved, then trypsinized to suspend them, supplemented with RPMI medium, and inserted into a 5-ml syringe. We used a portable imaging flow chamber (Ibidi, μ -Slide VI 0.1) containing a micro-fluidic channel (1 mm width, 17 mm length, 0.1 mm height). The 5-ml syringe containing the cells was connected to the chamber using a compatible tube (Ibidi, SN. 10831) and adapters (Ibidi, SN. 10825), and taped to the optical breadboard to ensure stability of the system. Another syringe and tube were attached to the other side of the flow chamber, to

withhold the excess cells and medium. Cells were then quantitatively imaged without labeling using the FI module, with the resulting OPD map shown in Fig. 5, and the coinciding video shown in [Visualization 1](#).

To conclude, we have presented an off-axis FI module, which is used for quantitative phase microscopy of biological cells. The module is simple, highly compact, inexpensive, easy to align, but still provides imaging of dense samples, and allows controlling the off-axis angle between the interferometric beams to optimally fit the spatial frequency of the interference fringes to the digital camera. This module is expected to work with partial temporal-coherence light sources, provided that beam path matching is obtained between the interferometric arms. However, this module is not expected to work with partial spatial-coherence light sources, due to the fact that flipping the FOV is carried out only in one of the interferometric arms. In the presented technique, the optical FOV is assumed to be at least two times wider than the digital FOV, and half of the optical FOV is assumed not to contain spatial sample information, a condition that is easily met for many biological samples including micro-fluidic channels containing biological cells. We thus expect this module to be integrated into existing micro-fluidic systems, enabling rapid quantitative cell visualization during flow, which might be useful for perspective cell sorting techniques.

Funding. U.S.–Israel Binational Science Foundation (BSF) (2013341); National Science Foundation (NSF) (ECCS 1545687).

Acknowledgment. We thank Dr. Ksawery Kalinowski and Yarden Mazor from Tel Aviv University for useful discussions. B. Javidi is supported by NSF ECCS (1545687).

REFERENCES

1. T. Blasi, H. Hennig, H. D. Summers, F. J. Theis, J. Cerveira, J. Patterson, D. Davies, A. Filby, A. E. Carpenter, and P. Rees, *Nat. Commun.* **7**, 10256 (2016).
2. S. Przibilla, S. Dartmann, A. Vollmer, S. Ketelhut, B. Greve, G. Bally, and B. Kemper, *J. Biomed. Opt.* **17**, 0970011 (2012).
3. G. Popescu, T. Ikeda, R. R. Dasari, and M. S. Feld, *Opt. Lett.* **31**, 775 (2006).
4. B. H. Bai, M. Shan, Z. Zhong, L. Guo, and Y. Zhan, *Opt. Laser Eng.* **75**, 1 (2015).
5. V. Mico, C. Ferreira, Z. Zalevsky, and J. García, *Opt. Express* **22**, 14929 (2014).
6. K. R. Lee and Y. K. Park, *Opt. Lett.* **39**, 3630 (2014).
7. S. Karepov, N. T. Shaked, and T. Ellenbogen, *Opt. Lett.* **40**, 2273 (2015).
8. J. Jang, C. Y. Bae, J. K. Park, and J. C. Ye, *Opt. Lett.* **35**, 514 (2010).
9. B. Kemper, A. Vollmer, C. E. Rommel, J. Schnekenburger, and G. von Bally, *J. Biomed. Opt.* **16**, 026014 (2011).
10. A. S. G. Singh, A. Anand, R. A. Leitgeb, and B. Javidi, *Opt. Express* **20**, 23617 (2012).
11. V. Chhaniwal, A. S. G. Singh, R. A. Leitgeb, B. Javidi, and A. Anand, *Opt. Lett.* **37**, 5127 (2012).
12. I. Moon, A. Anand, M. Cruz, and B. Javidi, *IEEE Photon.* **5**, 6900207 (2013).
13. P. Girshovitz and N. T. Shaked, *Opt. Express* **21**, 5701 (2013).
14. S. Mahajan, V. Trivedi, P. Vora, V. Chhaniwal, B. Javidi, and A. Anand, *Opt. Lett.* **40**, 3743 (2015).
15. P. Girshovitz and N. T. Shaked, *Opt. Express* **23**, 8773 (2015).
16. D. C. Ghiglia and M. D. Pritt, *Two-Dimensional Phase Unwrapping: Theory, Algorithms, and Software* (Wiley, 1998).